Original scientific paper

THERMAL BUCKLING ANALYSIS OF FUNCTIONALLY GRADED CIRCULAR PLATE RESTING ON THE PASTERNAK ELASTIC FOUNDATION VIA THE DIFFERENTIAL TRANSFORM METHOD

UDC 624.04

Fatemeh Farhatnia[1], Mahsa Ghanbari-Mobarakeh[1], Saeid Rasouli-Jazi[1], Soheil Oveissi[2]

[1]Department of Mechanical Engineering, Khomeinishahr Branch, Islamic Azad University, Khomeinishahr, Iran
[2]Department of Mechanical Engineering, Najafabad Branch, Islamic Azad University, Najafabad, Iran

Abstract. *In this paper, we propose a thermal buckling analysis of a functionally graded (FG) circular plate exhibiting polar orthotropic characteristics and resting on the Pasternak elastic foundation. The plate is assumed to be exposed to two kinds of thermal loads, namely, uniform temperature rise and linear temperature rise through thickness. The FG properties are assumed to vary continuously in the direction of thickness according to the simple power law model in terms of the volume fraction of two constituents. The governing equilibrium equations in buckling are based on the Von-Karman nonlinearity. To obtain the critical buckling temperature, we exploit a semi-numerical technique called differential transform method (DTM). This method provides fast accurate results and has a short computational calculation compared with the Taylor expansion method. Furthermore, some numerical examples are provided to consider the influence of various parameters such as volume fraction index, thickness-to-radius ratio, elastic foundation stiffness, modulus ratio of orthotropic materials and influence of boundary conditions. In order to predict the critical buckling temperature, it is observed that the critical temperature can be easily adjusted by appropriate variation of elastic foundation parameters and gradient index of FG material. Finally, the numerical results are compared with those available in the literature to confirm the accuracy and reliability of the DTM to determine the critical buckling temperature.*

Key Words: *Thermal Buckling, Orthotropic Plate, Functionally Graded Materials (FGM), Pasternak Elastic Foundation, Differential Transform Method (DTM)*

1. INTRODUCTION

One of the most important undesired phenomena in a mechanical structure as observed in plates is thermal buckling. The response of the plate to buckling depends on its mechanical properties. Functionally graded materials (FGM) are made of ceramic and metal constituents, including high mechanical strength, good machinery ability, and high thermal resistance. FGMs are a good choice to be employed as the material constituents in a plate exposed to high thermal gradients. They are less likely to delaminate at high temperatures due to the continuity of their physical and mechanical properties. In addition, the orthotropic properties of FGMs have received great attention because they increase the tolerance of plates to various types of loading. Numerous studies have been conducted on thermal plate buckling. In what follows, we mention the studies related to the subject of this paper. Dewey and Costello [1] proposed an analytical and experimental method to investigate the thermal buckling of flat plates where the modulus of elasticity changes due to the thermal gradient. Najafizadeh and Eslami [2] discussed the thermo-mechanical response of plates based on the first-order shear deformation theory. They derived nonlinear and linear governing equations from the energy method and by using the calculus of variations. In another work, Najafizadeh and Eslami [3] discussed the thermoelastic buckling of the circular orthotropic composite plates under various kinds of thermal loading. They obtained the governing equations based on the Love-Kirchhoff hypothesis and the Sanders' nonlinear strain-displacement relation. Li et al. [4] examined the nonlinear vibration and thermal buckling of orthotropic annular plates with a centric rigid mass. They employed the Hamilton's principle to derive the governing equations based on the Von-Karman nonlinearity. Najafizadeh and Heydari [5] assessed the thermal buckling of circular plates in functionally graded materials under uniform radial compression subject to various types of thermal loads. They established the governing equations in buckling, using variational method and solved them via Bessel functions. Prakash and Ganapathy [6] applied the finite element method to analyze the vibrations and thermal buckling of circular FGM plates. Zhao et al. [7] studied the thermal and mechanical buckling behavior of plates with arbitrary geometry, including plates containing square and circular holes in the center. Zenkour and Sobhy [8] investigated the thermal buckling of FG sandwich plates, using sinusoidal shear deformation plate theory. The thermal loads are assumed to have uniform, linear, and non-linear distribution through thickness. Jalali et al. [9] assessed the thermal buckling of circular FGM plates with varying thickness, using the pseudo-spectral method (PSM). Evaluating the reaction of plates resting on elastic foundations and subject to different types of loads has a great scientific importance, particularly in modern engineering structures. Kiani and Eslami [10] studied the exact solution of thermal buckling in annular FGM plates resting on the Pasternak elastic foundation. They examined the effects of geometrical parameters, power-law index, and coefficients of the elastic foundation on the critical buckling temperature. Jabbari et al. [11] studied the buckling of a solid porous circular plate subjected to thermal loading. They derived the governing equations based on the Sanders' nonlinear strain-displacement relation and determined the pre-buckling temperatures and the critical buckling temperatures. Yaghoobi and Fereidoon [12] proposed the thermal and mechanical buckling of functionally graded (FG) plates resting on elastic foundation, using nth-order shear deformation theory. They obtained the governing equations via exploiting the minimum total potential energy method. Mansouri and Shariat [13] predicted the thermal buckling response of heterogeneous orthotropic plates based on

the high-order theories. They employed a new version of the DQM (Differential Quadrature Method) to solve the governing differential equations. Mirzaei and Kiani [14] investigated the thermally induced bifurcation buckling of rectangular composite plates reinforced with single-walled carbon nanotubes. They revealed that in most cases, the FG-X pattern of CNTs is the most influential case since it results in higher critical buckling temperatures. Yu *et al.* [15] evaluated the new numerical results of thermal buckling of functionally graded plates (FGPs) with internal defects (for example, crack or cutout), using an effective numerical method. They employed the new formulation of the first-order shear deformation plate theory associated with extended isogeometric analysis (XIGA) and level sets. Moreover, they investigated the influences of various aspect ratios, including gradient index, crack length, plate thickness, cutout size, and boundary conditions on the critical buckling temperature rise (CBTR). Tung [16] studied the nonlinear bending and post-buckling behavior of functionally graded sandwich plates resting on elastic foundations and subject to uniform external pressure, thermal loading, and uniaxial compression in the thermal environment. Sun *et al.* [17] numerically investigated the thermomechanical buckling and post-buckling of a functionally graded material (FGM) Timoshenko beam resting on a two-parameter non-linear elastic foundation and subject to only a temperature rise, using the shooting method.

In the present research, we accomplish the thermal buckling of an orthotropic FG circular plate. To that end, the Differential Transformation Method (DTM) is applied to solve the governing equation of thermal buckling. The literature review indicates that the present work is the first attempt to exploit DTM to evaluate the critical buckling temperature. A number of studies have been carried out by this method [18-24]. The results are presented in four categories based on linear and uniform thermal load and simply supported and clamped edge conditions in the proceeding sections. The effects of parameters such as volume fraction index, stiffness of the Pasternak elastic foundation, thickness-to-radius ratio, and modulus ratio of orthotropic material to critical temperature are also investigated.

2. Mathematical Formulation of Constitutive Equations

Consider a functionally graded circular solid supported on the Pasternak elastic foundation (Fig. 1). A polar coordinate system (r, θ, z) is employed to label the material points of the plate in radial, circumferential, and thickness directions.
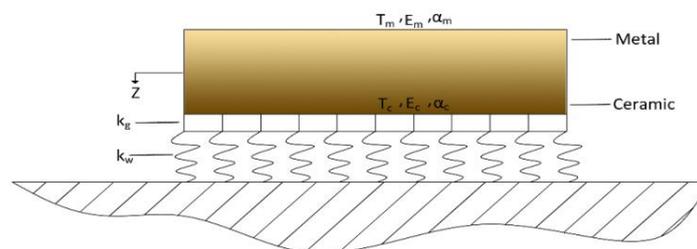
Fig. 1 Schematic of problem

Based on the Sanders' kinematic relations and the Von-Karman nonlinear assumption, the strain-displacement relationships are written in polar coordinates system as follows:

$$\varepsilon_{rr} = \overline{\varepsilon}_{rr} + zk_{rr}, \qquad \varepsilon_{\theta\theta} = \overline{\varepsilon}_{\theta\theta} + zk_{\theta\theta}, \qquad \gamma_{r\theta} = \overline{\gamma}_{r\theta} + 2zk_{r\theta} \qquad (1)$$

where $\overline{\varepsilon}_{rr}$, $\overline{\varepsilon}_{\theta\theta}$, and $\overline{\gamma}_{r\theta}$ are mid-surface strains and k_{rr}, $k_{\theta\theta}$, and $k_{r\theta}$ are the curvatures defined as follows:

$$\overline{\varepsilon}_{rr} = \frac{\partial u}{\partial r} + \frac{1}{2}\left(\frac{\partial w}{\partial r}\right)^2, \; k_{rr} = -\frac{\partial^2 w}{\partial r^2}$$

$$\overline{\varepsilon}_{\theta\theta} = \frac{1}{r}\frac{\partial v}{\partial \theta} + \frac{u}{r} + \frac{1}{2r^2}\left(\frac{\partial w}{\partial \theta}\right)^2, \; k_{\theta\theta} = -\frac{1}{r}\frac{\partial w}{\partial r} + \frac{1}{r^2}\frac{\partial^2 w}{\partial \theta^2} \qquad (2)$$

$$\overline{\gamma}_{r\theta} = \frac{1}{r}\frac{\partial u}{\partial \theta} + \frac{\partial v}{\partial r} - \frac{v}{r} + \frac{1}{r}\left(\frac{\partial w}{\partial r}\right)\left(\frac{\partial w}{\partial \theta}\right), \; k_{r\theta} = \frac{1}{r^2}\frac{\partial w}{\partial \theta} - \frac{1}{r}\frac{\partial^2 w}{\partial r\partial \theta}$$

where u, v, and w represent the middle-plane displacements in the polar coordinates. Stress-strain relationships in polar coordinates are expressed as follows:

$$\sigma_{rr} = a_{11}(\varepsilon_{rr} - (\varepsilon_T)_{rr}) + a_{12}(\varepsilon_{\theta\theta} - (\varepsilon_T)_{\theta\theta})$$

$$\sigma_{\theta\theta} = a_{21}(\varepsilon_{rr} - (\varepsilon_T)_{rr}) + a_{22}(\varepsilon_{\theta\theta} - (\varepsilon_T)_{\theta\theta}) \qquad (3)$$

$$\tau_{r\theta} = a_{66}\gamma_{r\theta}$$

in which,

$$a_{11} = \frac{E_r(z)}{1 - \vartheta_{r\theta}\vartheta_{\theta r}}, \quad a_{21} = \frac{\vartheta_r E_\theta(z)}{1 - \vartheta_{r\theta}\vartheta_{\theta r}}, \quad a_{12} = \frac{\vartheta_\theta E_r(z)}{1 - \vartheta_{r\theta}\vartheta_{\theta r}} \quad a_{22} = \frac{E_\theta(z)}{1 - \vartheta_{r\theta}\vartheta_{\theta r}},$$

$$a_{66} = G_{r\theta}, \quad \frac{\vartheta_{r\theta}}{E_r(z)} = \frac{\vartheta_{\theta r}}{E_\theta(z)}, \quad \beta = \frac{\alpha_\theta}{\alpha_r}, \qquad (4)$$

$$(\varepsilon_T)_{rr} = \alpha_r\Delta T, \quad (\varepsilon_T)_{\theta\theta} = \alpha_\theta\Delta T, \quad \Delta T = T - T_0$$

where ε_T is the thermal strain, α_r and α_θ are the thermal expansion coefficients in radial and circumferential directions, respectively. Moreover, T and T_0 are the current and reference temperatures, respectively. The readers interested in the thermo-elastic stress-strain relations in a symmetrical case of deformation can find more details in the study conducted by Kiani et al. [10]. Upon substituting Eq. (4) into Eq. (3), the constitutive relations for orthotropic FG plate can be re-written as follows:

$$\sigma_{rr} = a_{11}\varepsilon_{rr} + a_{12}\varepsilon_{\theta\theta} - (a_{11}\alpha_r + a_{12}\alpha_\theta)\Delta T$$

$$\sigma_{\theta\theta} = a_{21}\varepsilon_{rr} + a_{22}\varepsilon_{\theta\theta} - (a_{21}\alpha_r + a_{22}\alpha_\theta)\Delta T \qquad (5)$$

$$\tau_{r\theta} = a_{66}\gamma_{r\theta}$$

In addition, $G_{r\theta}$ is shear modulus, and E_r and E_θ are Young's modulus of the plate in radial and circumferential directions, respectively. Based on the power-law model in polar coordinates, the material properties are as follows:

$$E_r(z) = E_{rcm}(\frac{1}{2} + \frac{z}{h})^n + E_{rm}, \qquad E_{rcm} = E_{rc} - E_{rm} \qquad (6)$$

$$\alpha_r(z) = \alpha_{rcm}(\frac{1}{2} + \frac{z}{h})^n + \alpha_{rm}, \; \alpha_{rcm} = \alpha_{rc} - \alpha_{rm} \qquad (7)$$

$$\alpha_\theta(z) = \alpha_{\theta cm}(\frac{1}{2}+\frac{z}{h})^n + \alpha_{\theta m}, \qquad \alpha_{\theta cm} = \alpha_{\theta c} - \alpha_{\theta m} \tag{8}$$

$$G_{r\theta}(z) = G_{r\theta cm}(\frac{1}{2}+\frac{z}{h})^n + G_{r\theta m}, \qquad G_{r\theta cm} = G_{r\theta c} - G_{r\theta m} \tag{9}$$

where h, n and subscripts m and c represent the thickness, FG power index, the metal and ceramic properties, respectively. By assuming the polar orthotropic characteristics of plate, Young's modulus in the circumferential coordinate is defined as follows:

$$E_\theta(z) = \mu E_r(z) \Rightarrow E_\theta(z) = \mu(E_{cm}\left(\frac{1}{2}+\frac{z}{h}\right)^n + E_m) \tag{10}$$

where μ is the orthotropic modulus ratio.

3. GOVERNING EQUATIONS IN THERMAL BUCKLING

Stress resultants and stress couples are obtained as follows:

$$(N_{rr}, N_{\theta\theta}, N_{r\theta}) = \int_{-\frac{h}{2}}^{\frac{h}{2}} (\sigma_{rr}, \sigma_{\theta\theta}, \sigma_{r\theta})dz \tag{11}$$

$$(M_{rr}, M_{\theta\theta}, M_{r\theta}) = \int_{-\frac{h}{2}}^{\frac{h}{2}} z(\sigma_{rr}, \sigma_{\theta\theta}, \sigma_{r\theta})dz \tag{12}$$

Substituting Eq. (5) into Eqs. (11) and (12) yields the stress resultants and stress couples as follows:

$$N_{rr} = A_1\bar\varepsilon_{rr} + B_1 k_{rr} + A_2\bar\varepsilon_{\theta\theta} + B_2 k_{\theta\theta} - C_1\Delta T \tag{13}$$

$$N_{\theta\theta} = A_2\bar\varepsilon_{rr} + B_2 k_{rr} + A_3\bar\varepsilon_{\theta\theta} + B_3 k_{\theta\theta} - C_2\Delta T \tag{14}$$

$$M_{rr} = B_1\bar\varepsilon_{rr} + D_1 k_{rr} + B_2\bar\varepsilon_{\theta\theta} + D_2 k_{\theta\theta} - C_3\Delta T \tag{15}$$

$$M_{\theta\theta} = B_2\bar\varepsilon_{rr} + D_2 k_{rr} + B_3\bar\varepsilon_{\theta\theta} + D_3 k_{\theta\theta} - C_4\Delta T \tag{16}$$

where,

$$\begin{bmatrix} A_1 & A_2 & A_3 \\ B_1 & B_2 & B_3 \\ D_1 & D_2 & D_3 \end{bmatrix} = \int_{-\frac{h}{2}}^{\frac{h}{2}} \begin{bmatrix} 1 \\ z \\ z^2 \end{bmatrix} \begin{bmatrix} a_{11} & a_{12} & a_{22} \end{bmatrix} dz$$

$$(C_1, C_3) = \int_{-\frac{h}{2}}^{\frac{h}{2}} (1, z)(a_{11}\alpha_r + a_{12}\alpha_\theta)dz , \qquad (C_2, C_4) = \int_{-\frac{h}{2}}^{\frac{h}{2}} (1, z)(a_{21}\alpha_r + a_{22}\alpha_\theta)dz$$

When the plate is subjected to the mechanical loading, the total energy is given by:

$$V = U + \Omega \tag{17}$$

where Ω and U are the potential energy of the external loading and the strain energy, respectively. Ω is the summation of the potential energy of mechanical loading and two parameters elastic foundation reaction. The elastic foundation is exerted on the lower surface of the plate, as shown in Fig. 1. In this research, the mechanical loading is absent. U is the summation of thermal strain energy, membrane strain energy, bending strain energy, coupled bending-membrane strain energy, and elastic foundation strain energy:

$$U = \int_0^{2\pi} \int_0^R \int_{-h/2}^{h/2} \frac{1}{2} (\sigma_{rr}\varepsilon_{rr} + \sigma_{\theta\theta}\varepsilon_{\theta\theta} + \sigma_{r\theta}\varepsilon_{r\theta} - \sigma_{rr}\alpha_r\Delta T - \sigma_{\theta\theta}\alpha_\theta\Delta T)r dz dr d\theta \tag{18}$$

By integrating through thickness, U can be expressed as follows:

$$U = \int_0^{2\pi} \int_0^R \frac{1}{2} (\bar{\varepsilon}_r N_{rr} + k_{rr} M_{rr} + \bar{\varepsilon}_{\theta\theta} N_{\theta\theta} + k_{\theta\theta} M_{\theta\theta} + \bar{\gamma}_{r\theta} N_{r\theta} + 2k_{r\theta} M_{r\theta}$$
$$+ k_w w^2 + k_g \left(\frac{\partial w}{\partial r}\right)^2 + \frac{1}{r^2} k_g \left(\frac{\partial w}{\partial \theta}\right)^2)r dr d\theta \tag{19}$$

where k_w and k_g denote the stiffness of Pasternak elastic foundation (tension and shear foundation parameters, respectively). By substituting Eqs. (13-16) into Eq. (19), setting the resultant expression into the expression of the total potential energy function, Eq. (17), and employing Euler equations [5], the governing equilibrium equations in the buckling of the plate resting on the Pasternak foundation based on the von-Karman nonlinearity are obtained as follows [10]:

$$N_{r,r} + \frac{1}{r} N_{r\theta,\theta} + \frac{N_r - N_\theta}{r} = 0$$

$$N_{r\theta,r} + \frac{1}{r} N_{\theta,\theta} + \frac{2}{r} N_{r\theta} = 0 \tag{20}$$

$$M_{r,rr} + \frac{2}{r} M_{r,r} + \frac{1}{r^2} M_{\theta,\theta\theta} - \frac{1}{r} M_{\theta,r} + \frac{2}{r} M_{r\theta,r\theta} + \frac{2}{r^2} M_{r\theta,\theta} - N_r w_{,rr}$$
$$- N_\theta (\frac{1}{r^2} w_{,\theta\theta} + \frac{1}{r} w_{,r}) - k_w w + k_g (\frac{1}{r} w_{,r} + w_{,rr} + \frac{1}{r^2} w_{,\theta\theta}) = 0$$

The governing equations of equilibrium can be expressed in terms of displacement components by assuming the symmetric state of buckling which gives the variation with respect to the circumferential direction set to zero, substituting Eqs. (13-16) into Eqs. (20), and utilizing Eq. (2):

$$\frac{1}{(1-kv_r^2)} \left\{ E_1 \left[\frac{\partial^2 u}{\partial r^2} + \frac{1}{r}\frac{\partial u}{\partial r} - \frac{\mu u}{r^2} + \frac{\partial^2 w}{\partial r^2}\frac{\partial w}{\partial r} + \frac{(1-kv_r)}{2r}\left(\frac{\partial w}{\partial r}\right)^2 \right] \right.$$
$$\left. + E_2 \left[-\frac{\partial^3 w}{\partial r^3} - \frac{1}{r}\frac{\partial^2 w}{\partial r^2} + \frac{\mu}{r^2}\frac{\partial w}{\partial r} \right] \right\} + \frac{N_\theta^T - N_r^T}{r} = 0 \tag{21}$$

$$\frac{1}{(1-k\nu_r^{\ 2})}\left\{E_2\left[\frac{\partial^3 u}{\partial r^3}+\frac{2}{r}\frac{\partial^2 u}{\partial r^2}-\frac{\mu}{r^2}\frac{\partial u}{\partial r}+\frac{\mu u}{r^3}+\frac{\partial^3 w}{\partial r^3}\frac{\partial w}{\partial r}+\left(\frac{\partial^2 w}{\partial r^2}\right)^2+\frac{(2-k\nu_r)}{r}\frac{\partial^2 w}{\partial r^2}\frac{\partial w}{\partial r}\right]\right.$$

$$\left.+E_3\left[-\frac{\partial^4 w}{\partial r^4}-\frac{2}{r}\frac{\partial^3 w}{\partial r^3}+\frac{\mu}{r^2}\frac{\partial^2 w}{\partial r^2}-\frac{\mu}{r^3}\frac{\partial w}{\partial r}\right]\right\}+N_r^T w_{,rr}+\frac{1}{r}N_\theta^T w_{,r} \qquad (22)$$

$$-k_w w+k_g\left(\frac{1}{r}w_{,r}+w_{,rr}\right)=0$$

where,

$$E_1=h\left[E_m+\frac{E_{cm}}{n+1}\right],E_2=h^2 E_{cm}\left[\frac{1}{n+2}-\frac{1}{2n+2}\right],$$

$$E_3=h^3\left[\frac{E_m}{12}+E_{cm}\left[\frac{1}{n+3}+\frac{1}{4n+4}-\frac{1}{n+2}\right]\right]$$

3.1. Types of thermal loading

In this study, two cases of temperature rise are considered: uniform and linear temperature differences. When the plate is not thick enough, the assumption of linear distribution is reasonable [10]. But when the temperature on the top and bottom surfaces of the plate is constant and no source of heat is available in it, the temperature variation can be defined as a linear function of thickness coordinate; for instance, the temperature distribution in aircraft window, walls of the building, or furnace. By assuming that the reference temperature of plate is T_0 and the displacement in the radial direction is prevented due to restraint on the edge of the plate, N^T_r and N^T_θ as the representatives of stress resulting from the thermal gradients can be determined in two categories due to the temperature rise across thickness as follows:

− Uniform thermal loading:

$$N_r^T=C_1\Delta T=h\frac{(1+\beta\mu\nu_r)}{(1-\mu\nu_r^{\ 2})}\left[E_m\alpha_m+\frac{E_{cm}\alpha_m+E_m\alpha_{cm}}{n+1}+\frac{E_{cm}\alpha_{cm}}{2n+1}\right]\Delta T \qquad (23)$$

$$N_\theta^T=C_2\Delta T=h\frac{(\beta\mu+\mu\nu_r)}{(1-\mu\nu_r^{\ 2})}\left[E_m\alpha_m+\frac{E_{cm}\alpha_m+E_m\alpha_{cm}}{n+1}+\frac{E_{cm}\alpha_{cm}}{2n+1}\right]\Delta T \qquad (24)$$

− U Linear thermal loading:

$$T(z)=T_m+(T_c-T_m)\left(\frac{1}{2}+\frac{z}{h}\right) \qquad (25)$$

$$N_r^T=h\frac{(1+\beta\mu\nu_r)}{(1-\mu\nu_r^{\ 2})}(T_m-T_0)\left[E_m\alpha_m+\frac{E_{cm}\alpha_m+E_m\alpha_{cm}}{n+1}+\frac{E_{cm}\alpha_{cm}}{2n+1}\right]$$

$$+h\frac{(1+\beta\mu\nu_r)}{(1-\mu\nu_r^{\ 2})}\left[\frac{E_m\alpha_m}{2}+\frac{E_{cm}\alpha_m+E_m\alpha_{cm}}{n+2}+\frac{E_{cm}\alpha_{cm}}{2n+2}\right]\Delta T \qquad (26)$$

$$N_\theta^T = h\frac{(\beta\mu + \mu\nu_r)}{(1-\mu\nu_r^2)}(T_m - T_0)\left[E_m\alpha_m + \frac{E_{cm}\alpha_m + E_m\alpha_{cm}}{n+1} + \frac{E_{cm}\alpha_{cm}}{2n+1}\right]$$
$$+ \frac{h(\beta\mu+\mu\nu_r)}{(1-\mu\nu_r^2)}\left[\frac{E_m\alpha_m}{2} + \frac{E_{cm}\alpha_m + E_m\alpha_{cm}}{n+2} + \frac{E_{cm}\alpha_{cm}}{2n+2}\right]\Delta T \quad (27)$$

where $\Delta T=T(z)-T_0$. By eliminating the radial displacement components of u and after performing some mathematical manipulations, the equations of the equilibrium can be summarized in one equation in terms of out-plane displacement component of w as follows:

$$D_E\left[\frac{\partial^4 w}{\partial r^4} + \frac{2}{r}\frac{\partial^3 w}{\partial r^3} - \frac{\mu}{r^2}\frac{\partial^2 w}{\partial r^2} + \frac{\mu}{r^3}\frac{\partial w}{\partial r}\right] + (N_r^T + k_g)\frac{\partial^2 w}{\partial r^2} + \frac{1}{r}(N_\theta^T + k_g)\frac{\partial w}{\partial r} - k_w w = 0 \quad (28)$$

where, $D_E = (E_2^2 - E_1 E_3)/\mathrm{E}_1(1-\mu\upsilon_r^2)$. Based on the adjacent equilibrium criteria, the state of stable equilibrium may be designated by w_0; in addition, it is w_0+w_1 in the neighborhood of stability state when w_1 can be represented to any small increment of displacement. Similar to out-plane displacement, the stress resultants are divided into two terms representing the stable equilibrium and the neighboring state [10]. Upon substituting w_0+w_1 and stress resultants in two terms into the governing equation (28) and performing some mathematical manipulations, the stability equation is obtained as follows:

$$D_E\left[\frac{\partial^4 w_1}{\partial r^4} + \frac{2}{r}\frac{\partial^3 w_1}{\partial r^3} - \frac{\mu}{r^2}\frac{\partial^2 w_1}{\partial r^2} + \frac{\mu}{r^3}\frac{\partial w_1}{\partial r}\right] + (N_{r0}^T + k_g)\frac{\partial^2 w_1}{\partial r^2}$$
$$+ \frac{1}{r}(N_{\theta0}^T + k_g)\frac{\partial w_1}{\partial r} - k_w w_1 = 0 \quad (29)$$

where N_{r0}^T and $N_{\theta0}^T$ are the pre-buckling thermal loading, and the following relation can be established: $N_{r0}^T = N_{\theta0}^T = -N^T$. The following dimensionless quantities are defined to deal with the problem under consideration in the dimensionless forms:

$$\Phi = \frac{w_1}{h}, \quad \xi = \frac{r}{R}, \quad n_r^T = \frac{N_r^T R^2}{D_E}, \quad n_\theta^T = \frac{N_\theta^T R^2}{D_E}, \quad K_g = \frac{k_g R^2}{D_E}, \quad K_w = \frac{k_w R^4}{D_E}$$

$$\xi^3\frac{d^4\Phi}{d\xi^4} + 2\xi^2\frac{d^3\Phi}{d\xi^3} - \mu\xi\frac{d^2\phi}{d\xi^2} + \mu\frac{d\Phi}{d\xi} + (n_r^T + K_g)\xi^3\frac{d^2\Phi}{d\xi^2}$$
$$+ (n_\theta^T + K_g)\xi^2\frac{d\Phi}{d\xi} - K_w\xi^3\Phi = 0 \quad (30)$$

4. SOLVING THE GOVERNING EQUATION BY DTM

The differential transform method (DTM) is a numerical method based on the Taylor series expansion that proposes the solution in the form of polynomials [24]. This method is a fast convergent method in comparison with the Taylor series in order to solve the differential equations. The advantage of this method is its low computational manipulation and its applicability to handle linear and non-linear ordinary and partial differential equations. By

exploiting the DTM, the differential equations are reduced to the recurrence relations and convert the boundary conditions into a set of algebraic equations. The differential transform of the *k-th* derivative of function *f(r)* is defined as follows:

$$F[k] = \frac{1}{k!}\left(\frac{d^k f(r)}{dr^k}\right)_{r=r_0} \tag{31}$$

where *f(r)* and *F[k]* are the original function and transform function, respectively. The inverse differential transform of *F[k]* is defined as follows [5]:

$$f(r) = \sum_{k=0}^{\infty} F[k](r - r_0)^k \tag{32}$$

In the domain of R, original function *f(r)* is considered to be analytical, and $r=r_0$ represents any point in R. *f(r)* is represented by power series whose center is located at r_0. From Eqs. (31) and (32), it can be concluded that:

$$f(r) = \sum_{k=0}^{\infty} \frac{(r - r_0)^k}{k!}\left(\frac{d^k f(r)}{dr^k}\right)_{r=r_0} \tag{33}$$

Table 1 demonstrates the fundamental mathematical properties of the differential transform method (DTM):

Table 1 Fundamental theorems of DTM [22]

Original Function	Transformed Function
$f(r) = y(r) \pm z(r)$	$F[k] = Y[k] \pm Z[k]$
$f(r) = \lambda y(r)$	$F[k] = \lambda Y[k]$
$f(r) = y(r).z(r)$	$F[k] = \sum_{k_1=0}^{k} Y[K_1] \, Z[K - K_1]$
$f(r) = \frac{(d^m y(r))}{(dr^m)}$	$F[k] = \frac{(m+k)!}{k!} Y[k + m]$
$f(r) = r^n$	$F[k] = \delta(k - n) = \begin{cases} 0 & if \quad k \neq n \\ 1 & if \quad k = n \end{cases}$

Hence, function Φ[ξ] is obtained as follows:

$$\Phi[\xi] = \sum_{k=0}^{N} \phi[k]\xi^k = \phi[0]\xi^0 + \phi[1]\xi^1 + \phi[2]\xi^2 + \ldots \tag{34}$$

To solve Eq. (35), we use the differential transform relationships of the *k-th* derivative of the function of non-dimensional out-plane displacement Φ; moreover, DTM theorems are listed in Table 1:

$$\xi^3 \frac{d^4\Phi}{d\xi^4} = \sum_{k_1=0}^{k} \delta(k_1-3)(k-k_1+4)(k-k_1+3)(k-k_1+2)(k-k_1+1)\phi[k-k_1+4]$$

$$\xi^2 \frac{d^3\Phi}{d\xi^3} = \sum_{k_1=0}^{k} \delta(k_1-2)(k-k_1+3)(k-k_1+2)(k-k_1+1)\phi[k-k_1+3]$$

$$\xi \frac{d^2\Phi}{d\xi^2} = \sum_{k_1=0}^{k} \delta(k_1-1)(k-k_1+2)(k-k_1+1)\phi[k-k_1+2]$$

$$\frac{d\Phi}{d\xi} = (k+1)\phi[k+1] \tag{35}$$

$$\xi^3 \frac{d^2\Phi}{d\xi^2} = \sum_{k_1=0}^{k} \delta(k_1-3)(k-k_1+2)(k-k_1+1)\phi[k-k_1+2]$$

$$\xi^2 \frac{d\Phi}{d\xi} = \sum_{k_1=0}^{k} \delta(k_1-2)(k-k_1+1)\phi[k-k_1+1]$$

$$\xi^3 \Phi = \sum_{k_1=0}^{k} \delta(k_1-3)\phi[k-k_1]$$

Substituting the aforementioned relationships into the governing equation in thermal buckling Eq. (28) yields:

$$\sum_{k_1=0}^{k} \delta(k_1-3)(k-k_1+4)(k-k_1+3)(k-k_1+2)(k-k_1+1)\phi[k-k_1+4]$$

$$+2\sum_{k_1=0}^{k} \delta(k_1-2)(k-k_1+3)(k-k_1+2)(k-k_1+1)\phi[k-k_1+3]$$

$$-\mu\sum_{k_1=0}^{k} \delta(k_1-1)(k-k_1+2)(k-k_1+1)\varphi[k-k_1+2]+\mu(k+1)\phi[k+1] \tag{36}$$

$$+A_1\sum_{k_1=0}^{k} \delta(k_1-3)(k-k_1+2)(k-k_1+1)\phi[k-k_1+2]$$

$$+A_2\sum_{k_1=0}^{k} \delta(k_1-2)(k-k_1+1)\varphi[k-k_1+1]-K_w\sum_{k_1=0}^{k} \delta(k_1-3)\ \phi[k-k_1]=0$$

By utilizing the appropriate theorems of the DT method (see Table 1 and the simplified form of Eq. 36), we have the following recurrence relation:

$$\phi[k+1] = \frac{(A_1(k-2)+A_2)(k-1)\phi[k-1]-K_w\phi[k-3]}{(-k^2+\mu)(k^2-1)}, \qquad k \geq 3 \tag{37}$$

where $A_1=n^T_r+K_g$ and $A_2=n^T_\theta+K_g$.

The following boundary conditions are imposed as clamped and simply supported boundary conditions on the edges of the plate. However, by applying differential transformation method to boundary conditions, we can obtain:

- Non-dimensional clamped edge:

$$\phi\big|_{\xi=1} = 0 \ , \quad \frac{d\phi}{d\xi}\bigg|_{\xi=1} = 0 \tag{38}$$

- Differential transform of clamped edge condition with DTM:

$$\sum_{k=0}^{N} \phi[k] = 0, \quad \sum_{k=0}^{N} k\phi[k] = 0 \tag{39}$$

- Non-dimensional simply supported boundary condition:

$$\phi\big|_{\xi=1} = 0, \quad -D_E\left[\frac{d^2\phi}{d\xi^2} + \frac{v}{r}\frac{d\phi}{d\xi}\right]\bigg|_{\xi=1} = 0 \tag{40}$$

- Differential transform of simply supported edge condition with DTM:

$$\sum_{k=0}^{N} \phi[k] = 0, \quad \sum_{k=0}^{N} k(k-1+v)\phi[k] = 0 \tag{41}$$

In this study, the symmetrical thermal buckling behavior of a plate is considered, and the regularity condition is imposed besides the boundary conditions. The non-dimensional form of regularity condition and its differential transform are as follows:

$$\frac{d\phi}{d\xi}\bigg|_{\xi=0} = 0, \quad \phi[1] = 0 \tag{42}$$

Upon substituting $k=3,5,7,\ldots$ into the recurrence Eq. (37), we get:

$$\varphi[3] = -\frac{A_2\varphi[1]}{3\mu+12} = 0$$

$$\varphi[5] = \frac{(6A_1+3A_2)\varphi[3] - K_w\varphi[1]}{15\mu-240} = 0, \quad \varphi[7] = \frac{(20A_1+5A_2)\varphi[5] - K_w\varphi[3]}{35\mu-1260} = 0 , \ \ldots \tag{43}$$

It can be concluded that for odd values of k in Eq. (34), $\varphi[k]$ equals zero [23-24]. Therefore, by using recurrence Eq. (37), we can find that $\varphi[k]$ can be determined in terms of $\varphi[0]$ and $\varphi[2]$. By using recurrence relation (37) for $k=2, 4, 6,\ldots$, we can obtain the following equations:

$$\phi[4] = \frac{2(A_1+A_2)\phi[2] - K_w\phi[0]}{8\mu-72}$$

$$\phi[6] = \frac{(12A_1+4A_2)\phi[4] - K_w\phi[2]}{24\mu-600}, \quad \phi[8] = \frac{(30A_1+6A_2)\phi[6] - K_w\phi[4]}{48\mu-2352}, \ \ldots \tag{44}$$

Hence, all the $\varphi[k]$ with even values of k in Eq. (34) can be expressed in terms of $\varphi[2]$, $\varphi[0]$.

In order to determine the critical buckling temperature, recurrence relation (42) and imposed boundary conditions of Eq. (39) are simultaneously employed for clamped edges. Therefore, a set of two homogenous equations are established in terms of $\varphi[0]$ and $\varphi[2]$, as follows:

$$\begin{cases} H_{11}\phi[0] + H_{12}\phi[2] = 0 \\ H_{21}\phi[0] + H_{22}\phi[2] = 0 \end{cases} \tag{45}$$

where H_{11}, H_{12}, H_{21}, and H_{22} are the coefficients of polynomials of *N-th* order.

$$H_{11} = 1 - \frac{K_w}{8\mu - 72} - \frac{(3A_1 + A_2)K_w}{(6\mu - 150)(8\mu - 72)} + \cdots$$

$$H_{12} = 1 + \frac{A_1 + A_2}{4\mu - 36} - \frac{K_w}{24\mu - 600} + \frac{(3A_1 + A_2)(A_1 + A_2)}{(6\mu - 150)(4\mu - 36)} + \cdots$$

$$H_{21} = \frac{-K_w}{2\mu - 18} - \frac{6(3A_1 + A_2)K_w}{(6\mu - 150)(2\mu - 36)} + \cdots \tag{46}$$

$$H_{22} = 2 + \frac{A_1 + A_2}{\mu - 9} - \frac{K_w}{4\mu - 100} + \frac{(12A_1 + 4A_2)(A_1 + A_2)}{(4\mu - 100)(4\mu - 36)} + \cdots$$

For a non-trivial solution of Eq. (45), the determinant of coefficients must vanish, leading to the eigenvalue problem. Hence, we have:

$$\begin{vmatrix} H_{11} & H_{12} \\ H_{21} & H_{22} \end{vmatrix} = 0 \tag{47}$$

In a similar manner, we can obtain the solution for the simply supported plate by utilizing the recurrence relation (37) and the imposed boundary conditions of Eq. (41).

5. NUMERICAL RESULTS

In this section, some numerical results are presented for the thermal buckling of orthotropic FG circular plates of two categories of uniform and linear temperature rise under clamped and simply supported boundary conditions. Due to the high volume of the calculations required, the system of algebraic equations presented in the preceding section are implemented in a computer code in MATLAB software, and the numerical results are presented in a tabulated form. For the numerical results, an FG plate composed of aluminum (as metal) and alumina (as ceramic) is considered. Young's modulus of aluminum (Al) and alumina are E_m=70 *Gpa* and E_c=380 *Gpa*, respectively. The thermal expansion coefficients are α_m=23×10^{-6} K^{-1} and α_c=7.4×10^{-6} K^{-1} for metal and ceramic constituents, respectively. Poisson's ratio remains constant at v=0.3. It is assumed that the material properties are assumed to be temperature-independent. To examine the convergence rate of DT method, we obtain the results for a clamped isotropic homogeneous circular plate with the thickness-to-radius ratio of *h/R*=0.01. We observe that the number of terms (*k*=20) is sufficient to get precise values of the critical temperature. This trend remains constant in other numerical results as presented in the following section.

5.1. Uniform loading - clamped boundary condition

Table 2 shows the variation of the critical buckling temperature with respect to FG power-law index, thickness-to-radius ratio, and orthotropic ratio. As it is observed, the critical temperature increases as the value of μ rises. According to Table 2, for a specific *h/R* ratio, the buckling critical temperature is reduced by increasing the value of n; however, increasing the *h/R* ratio increases the values of the critical temperature.

Table 2 Variation of the critical temperature (^oK) of the clamped plate versus FG power-law index, orthotropic ratio, and thickness-to-radius ratio in case of uniform thermal loading

μ	*h/R*	*n* 0	0.5	1	2	5	10
0.50	0.010	7.070	4.081	3.163	2.914	2.151	2.002
	0.150	15.911	9.104	7.390	6.552	6.060	5.950
	0.020	28.280	16.081	12.851	11.652	11.141	10.860
	0.030	63.641	36.153	28.934	26.214	26.042	25.851
	0.040	113.132	64.214	52.560	46.603	46.142	45.823
0.70	0.010	13.780	7.813	6.422	5.684	5.164	5.010
	0.150	31.020	17.570	14.414	12.780	11.181	10.551
	0.020	55.131	31.232	25.611	22.714	21.421	21.090
	0.030	124.061	70.280	55.412	51.091	52.732	50.261
	0.040	220.552	124.944	98.503	90.831	93.721	92.361
0.9	0.010	21.381	12.112	9.5404	8.812	9.150	9.040
	0.150	48.110	27.260	21.480	19.823	20.444	20.121
	0.020	85.541	48.460	38.881	35.234	36.341	33.370
	0.030	192.462	109.033	89.412	79.270	81.841	80.124
	0.040	342.152	193.842	152.872	140.920	145.382	142.534
1	0.010	24.950	14.142	11.594	10.280	10.001	8.901
	0.150	56.150	31.813	25.083	23.132	21.863	20.520
	0.020	99.824	56.552	46.370	41.113	38.411	38.604
	0.030	224.581	127.240	104.343	92.504	89.432	88.104
	0.040	399.270	226.214	185.480	164.451	161.652	160.412
1.5	0.010	51.633	29.262	23.480	21.260	21.941	22.561
	0.150	114.280	64.744	53.091	47.120	48.562	49.933
	0.020	203.141	115.081	94.421	83.662	80.311	78.760
	0.030	456.602	258.660	213.192	188.150	194.121	199.480
	0.040	807.412	457.411	360.590	332.542	343.150	352.761
2	0.010	87.150	49.371	40.634	35.890	33.151	31.134
	0.150	200.051	113.361	89.381	82.393	78.050	77.412
	0.020	349.374	197.942	162.401	143.881	141.450	140.661
	0.030	794.632	450.160	355.991	327.270	322.644	320.180
	0.040	1408.221	797.630	651.631	579.880	558.262	555.180

Table 3 exhibits the critical buckling temperature with respect to elastic foundation coefficient, orthotropic ratio, and FG power-law index. As elastic foundation coefficients increase by increasing the orthotropic ratio, the critical temperature increases. On the other hand, when the FG power-law index increases, the critical temperature decreases. This shows that the pure ceramic plate, compared to the metal-ceramic plate, is more stable at the elevated working temperature.

Table 3 Variation of the critical temperature (^{o}K) of the clamped plate versus FG power-law index, orthotropic ratio, and elastic foundation on the critical temperature in case of uniform thermal loading, h/R=0.020

μ	n	k_w, k_g					
		(0,0)	(100,0)	(200,0)	(500,0)	(100,10)	(200,20)
0.7	0	55.131	63.121	67.341	81.470	77.470	96.911
	0.50	31.232	35.690	38.150	46.151	43.880	54.880
	1	25.611	29.341	31.280	37.851	35.903	44.841
	2	22.714	26.030	27.741	33.581	31.960	39.801
	5	21.422	23.822	24.633	31.610	30.841	37.250
1	0	99.824	114.293	121.780	147.531	140.050	175.360
	0.5	56.552	64.520	69.270	83.812	79.512	99.5281
	1	46.370	53.141	56.343	68.301	65.381	81.334
	2	41.113	47.282	50.480	61.012	57.722	73.982
	5	38.411	44.690	47.742	59.553	53.801	71.552
1.5	0	203.142	232.570	248.150	300.222	285.450	357.153
	0.5	115.081	131.764	140.580	170.244	161.711	202.300
	1	94.421	108.111	115.342	139.544	132.680	165.823
	2	83.662	95.781	102.233	123.644	117.583	147.221
	5	80.313	92.812	100.433	120.810	115.283	145.342

5.2. Linear loading - clamped boundary conditions

Table (4) represents the effect of increasing the thickness-to-radius ratio on increasing the critical temperature in case of linear thermal loading condition. This table clearly shows that the trend of variation of the critical temperature is confirmed in Table 2 as well. The comparison of the two tables indicates that the rate of increase is higher for linear thermal loading as compared to the uniform one. Nevertheless, for small h/R and non-zero quantities of n, this trend is reversed.

Table 4 Variation of the critical buckling temperature ($^\circ K$) for the clamped plate
in case of linear thermal loading, $(k_w, k_g)=0$

μ	h/r	n				
		0	0.5	1	2	5
0.50	0.010	8.480	2.652	0.843	0.351	0.305
	0.150	26.531	12.780	8.673	6.640	6.062
	0.020	50.740	26.521	19.272	15.472	14.763
	0.030	67.592	37.052	27.860	22.873	20.160
	0.040	220.670	122.801	93.292	77.060	73.893
0.70	0.010	15.173	4.750	1.511	0.523	0.451
	0.150	43.640	21.021	14.272	10.920	10.284
	0.020	93.142	48.682	35.372	28.403	27.932
	0.030	234.551	128.581	96.700	79.370	77.370
	0.040	432.540	240.714	182.851	151.231	150.681
0.9	0.010	22.772	7.123	2.274	0.650	0.563
	0.150	76.230	36.710	24.922	19.110	18.713
	0.020	151.082	78.962	57.371	46.122	44.920
	0.030	364.921	200.153	150.444	123.480	122.212
	0.040	664.300	369.6821	280.832	231.901	231.493
1	0.010	29.912	8.273	2.980	0.731	0.660
	0.150	92.291	43.632	30.171	23.101	21.860
	0.020	179.632	93.131	68.214	54.772	53.790
	0.030	429.171	234.563	176.932	145.231	143.053
	0.040	778.532	432.552	329.124	271.880	264.810
1.5	0.010	62.510	19.562	15.032	10.080	9.840
	0.150	197.501	95.113	71.954	57.064	55.860
	0.020	355.670	185.882	151.512	118.450	115.042
	0.030	931.304	510.520	390.711	322.131	315.793
	0.040	1572.631	875.182	671.040	555.614	551.260
2	0.010	101.694	31.813	30.290	22.394	21.350
	0.150	325.971	156.981	124.653	100.291	98.140
	0.020	617.394	322.672	251.290	205.614	205.380
	0.030	1511.632	828.650	639.903	528.782	524.433
	0.040	2266.591	1261.371	971.882	805.652	803.570

Table (5) shows the effect of the presence of elastic foundation on the critical buckling temperature for linear loading condition. As it is observed, the critical temperature decreases when the elastic foundation coefficient gets more values.

In order to validate the present solutions, we compare them with the results obtained from the study conducted by Ghiasian et al. [25]. Table (6) shows the critical temperature for the clamped plate without elastic foundation. The values are E_m=201 Gpa, α_m=12.33×10^{-6} K^{-1}, E_c=350 Gpa, and α_c=5.87×10^{-6} K^{-1}, and the Poisson's ratio is v=0.3.

Table 5 Effect of elastic foundation on the critical buckling temperature
for linear temperature rise, h/R=0.020

μ	n	(k_w, k_g)					
		(0,0)	(100,0)	(200,0)	(500,0)	(100,10)	(200,20)
	0	93.140	107.621	114.160	136.523	142.211	163.120
	0.50	48.681	56.560	60.163	71.362	74.610	54.442
	1	35.371	41.212	43.363	51.851	54.661	61.681
0.7	2	28.401	33.280	35.222	41.634	43.362	49.742
	5	27.931	33.111	35.022	41.411	43.331	48.040
	0	179.632	207.291	219.152	264.062	274.664	312.511
	0.5	93.131	105.611	111.761	134.290	141.562	158.322
	1	68.210	79.390	83.900	100.812	104.361	118.692
1	2	54.772	64.361	66.274	80.2380	85.331	117.322
	5	54.390	65.830	65.182	79.012	83.030	98.190
	0	355.670	416.954	439.520	521.322	545.123	622.433
	0.5	185.880	217.913	229.722	272.253	284.620	325.342
	1	151.510	177.622	187.244	222.363	234.163	265.253
1.5	2	118.450	138.863	146.370	173.632	180.853	207.283
	5	117.841	140.721	145.342	172.884	180.052	206.220

Table 6 Comparison of the results of the present study with those of Ref. [25]

	n	$\dfrac{h}{R}$							
		0.010	p.e.[*]	0.020	p.e.[*]	0.030	p.e.[*]	0.040	p.e.[*]
Present		12.731		49.910		112.291		199.644	
Ref. [25]	0	12.591	1.11	50.360	0.893	113.293	0.884	201.369	0.857
Present		9.532		37.001		83.142		141.149	
Ref. [25]	0.5	9.265	2.88	37.055	0.146	83.362	0.264	141.170	0.015
Present		8.536		33.120		74.921		133.358	
Ref. [25]	1	8.335	2.41	33.338	0.654	75.000	0.105	133.307	0.038
Present		7.761		30.554		68.752		122.314	
Ref. [25]	2	7.700	0.792	30.798	0.792	69.284	0.768	123.147	0.676
Present		7.370		28.486		64.326		114.452	
Ref. [25]	5	7.175	2.718	28.696	0.732	64.556	0.356	114.742	0.253

[*]The percentage of error

5.3. Effect of boundary conditions on the critical buckling temperature

In circular FG plates, due to the stretching-bending coupling exposed to uniform thermal loading, the asymmetric material distribution induces the pre-buckling thermal moments. Therefore, the bifurcation buckling may not occur, and the buckling critical temperature is not available [26]. However, the plates with clamped edges can tolerate the bending moments and remain in an un-deformed configuration. In this study, we consider that the variation of the critical buckling temperature is tabulated for a homogeneous orthotropic circular plate under simply supported boundary condition, as shown in Table 7.

Table 7 Variation of the critical buckling temperature for a homogeneous orthotropic circular plate under simply supported boundary condition and linear and uniform temperature rises

$\dfrac{h}{R}$	μ					
	0.50		0.70		0.90	
	Uniform	Linear	Uniform	Linear	Uniform	Linear
0.010	2.06	4.12	3.72	7.45	5.37	10.74
0.150	4.63	9.26	8.37	16.74	12.08	24.17
0.020	8.23	16.46	14.88	29.76	21.48	42.96
0.030	18.52	37.04	33.49	66.97	48.34	96.67
0.040	32.92	65.84	59.53	119.04	85.93	171.86
$\dfrac{h}{R}$	1.0		1.50		2.00	
	Uniform	Linear	Uniform	Linear	Uniform	Linear
0.010	6.03	12.07	10.31	20.76	15.80	34.28
0.150	13.58	27.15	23.29	46.24	39.64	79.55
0.020	24.13	48.27	41.46	73.41	70.46	126.31
0.030	54.30	108.60	93.10	187.88	159.56	318.12
0.040	96.54	193.08	165.95	333.14	253.41	569.59

6. CONCLUSIONS

In this paper, we have analyzed the thermal buckling of a circular FGM plate resting on the Pasternak elastic foundation and subjected to uniform and linear thermal loading by employing the differential transform method (DTM) to obtain the solutions. Some remarkable conclusions obtained in this study are as follows:

- By utilizing the differential transform method (DTM), the governing differential equation in the thermal buckling can be transformed to algebraic equations in the sub-domains. DTM is capable of deriving the analytical solution to determine the critical buckling temperature for FG orthotropic plate resting on two-parameter (Pasternak) foundations.
- Comparing the results with those existing in the literature indicates that DTM is a fast convergent, precise, and cost-efficient tool to analyze the thermal buckling behavior of functionally graded plates.

- By increasing volume fraction n, the flexural rigidity is reduced as the plate becomes more metal-rich. Consequently, the critical buckling temperature is reduced. This leads to the conclusion that for a ceramic-rich plate, the value of the critical temperature is the maximum.
- The present study has investigated the effect of the presence of elastic foundation, as a controlling parameter, on the critical temperature for two boundary conditions, namely clamped and simply supported edges. The numerical results indicate that increasing the parameters of elastic foundation increases the critical temperature. Hence, the critical temperature in buckling can be adjusted effectively.
- According to the results, when the temperature rises linearly, the critical temperature gets higher values in comparison with the uniform temperature rise.
- As the ratio of Young's modulus in the circumferential direction to that in the radial one increases, the plate demonstrates a more resistant behavior. Therefore, the critical buckling temperature increases.

REFERENCES

1. Dewey, B.R, Costello, G.A., 1968, *Thermal buckling of nonhomogeneous plates*, Nuclear Engineering and Design, 7(3), pp. 249-261.
2. Najafizadeh, M.M., Eslami, M.R., 2002, *First-order-theory-based thermoelastic stability of functionally graded material circular plate*, AIAA J, 40(7), pp.1444–1450.
3. Najafizadeh, M.M., Eslami, M.M., 2002 *Thermoelastic stability of orthotropic circular plates*, Journal of Thermal Stresses, 25(10), pp. 985-1005.
4. Li, S.R., Zhou, Y.H., Song, X., 2002, *Non-linear vibration and thermal buckling of an orthotropic annular plate with a centric rigid mass*, Journal of Sound and Vibration, 251(1), pp. 141-152.
5. Najafizadeh, M.M., Heydari, H.R., 2004, *Thermal buckling of functionally graded circular plates based on higher order shear deformation plate theory*, European Journal of Mechanics A/Solids., 23, pp. 1085–1100.
6. Prakash, T., Ganapathi, M., 2006, *Asymmetric flexural vibration and thermoelastic stability of FGM circular plates using finite element method*, Composites: Part B. Engineering, 37(7–8), pp.642–649.
7. Zhao, X., Lee, K.M., Liew, K.M., 2009, *Mechanical and thermal buckling analysis of functionally graded plates*, Composite Structure, 90(2), pp.161-17.
8. Zenkour, A.M., Sobhy, M., 2010, *Thermal buckling of various types of FGM sandwich plates*, Composite Structure, 93(1), pp. 93-102.
9. Jalali, S.K, Naei, M.H., Poorsolhjouy, A., 2010, *Thermal stability analysis of circular functionally graded sandwich plates of variable thickness using pseudo-spectral method*, Mater. Des., 31(10), pp.4755–63.
10. Kiani, Y., Eslami, M.R., 2013, *An exact solution for thermal buckling of annular FGM plates on an elastic medium*, Composites Part B: Engineering, 45(1), pp.101-110.
11. Jabbari, M., Hashemitaheri, M., Mojahedin, M.R., 2014, *Thermal Buckling Analysis of Functionally Graded Thin Circular Plate Made of Saturated Porous Materials*, Journal of Thermal Stresses, 37(2), pp. 202-220.
12. Yaghoobi, H., Fereidooni, A., 2014, *Mechanical and thermal buckling analysis of functionally graded plates resting on elastic foundations: An assessment of a simple refined nth-order shear deformation theory*, Composites Part B: Engineering, 62, pp. 11-26.
13. Mansouri, M.H., Shariyat, M., 2014, *Thermal buckling predictions of three types of high-order theories for the heterogeneous orthotropic plates, using the new version of DQM*, Composite Structure, 113, pp. 40-55.
14. Mirzaei, M., Kiani, Y., 2016, *Thermal buckling of temperature-dependent FG-CNT-reinforced composite plates*, Meccanica, 51(9), pp. 2185–2201
15. Yu, T., Bui, T.Q., Yin, S., Doan, D.H., Wu, C.T., Do, T.V., Tanaka, S., 2016, *On the thermal buckling analysis of functionally graded plates with internal defects using extended isogeometric analysis*, Composite Structures, 136, pp. 684–695.

16. Tung, H.V., 2015, *Thermal and thermomechanical post-buckling of FGM sandwich plates resting on elastic foundations with tangential edge constraints and temperature-dependent properties*, Composite Structures, 131(1), pp. 1028–1039.

17. Sun, Y., Li, S.R., Batra, R.C., 2016, *Thermal buckling and post-buckling of FG Timoshenko beams on nonlinear elastic foundation*, Journal of Thermal Stresses, 39(1), pp. 11-26.

18. Attarinejad, R., Semnani, Sh.J., Shahba, A., 2006, *Basic displacement functions for free vibration analysis of non-prismatic Timoshenko beams*, Journal of Finite Elements in Analysis and Design, 46 (10), pp. 916–929.

19. Ozdemir, O., Kaya, M.O., 2006, *Flap wise bending vibration analysis of a rotating tapered cantilever Bernoulli–Euler beam by differential transform method,* Journal of Sound and Vibration, 289, pp. 413–420.

20. Yalcin, H.S., Arikoglu, A., Ozkol, I., 2009, *Free vibration analysis of circular plates by differential transformation method*, Computational and Applied Mathematics, 212, pp.377–386.

21. Yeh, Y.L., Wang, C.C., Jang, M.J., 2007, *Using finite difference and differential transformation method to analyze of large deflections of orthotropic rectangular plate problem*, Applied Mathematics and Computation, 190(2), pp.1146-1156.

22. Abbasi, S., Farhatnia, F., Jazi, S. R., 2013, *Application of Differential Transformation Method (DTM) for bending Analysis of Functionally Graded Circular Plates*, Caspian Journal of Applied Sciences Research, 2(4), pp. 17-23.

23. Abbasi, S., Farhatnia, F., Jazi, S.R., 2014, *A semi-analytical solution on static analysis of circular plate exposed to non-uniform axisymmetric transverse loading resting on Winkler elastic foundation,* Archives of Civil and Mechanical engineering, 14, pp. 476-488.

24. Lai, R., Ahlawat, N., 2015, *Axisymmetric vibrations and buckling analysis of functionally graded circular plates via differential transform method*, European Journal of Mechanics A/Solids, 52, pp. 85-94.

25. Ghiasian, SE., Kiani, Y., Sadighi, M., Eslami, M.R., 2014, *Thermal buckling of shear deformable temperature dependent circular/annular FGM plates*, International journal of Mechanical Sciences, 81, pp.137-148.

26. Li, S., Zhang, J., Zhao, Y., 2007, *Nonlinear thermomechanical post-buckling of circular FGM plate with geometric imperfection*, Thin-Walled Structures, 45(5), pp. 528-536.